J. Fluid Mech. (1965), *vol.* 22, *part* 3, *pp.* 481–505
Printed in Great Britain

A study of the turbulent separated-flow region occurring at a compression corner in supersonic flow

By H. McDONALD

British Aircraft Corporation, Preston Division, Warton Aerodrome,
Near Preston, Lancashire

(Received 15 June 1964 and in revised form 12 January 1965)

The turbulent separated-flow region occurring at a compression corner under certain circumstances at supersonic speeds has been examined in the light of recent improvements to base pressure theory (McDonald 1964). This base pressure theory is further extended from what could be termed a single-layer model of the re-attaching boundary layer to a two-layer model, thus enabling the inviscid shock configuration which occurs at the corner to be determined. Application of this analysis to some experimental results indicates a substantial measure of agreement.

While this analysis has been framed for estimating the scale of the corner interaction, the extension can of course be applied to increase the range of initial boundary-layer thicknesses to which McDonald's analysis is applicable. An example of such an application is shown to be in good agreement with experiment.

1. Introduction

A sketch of the interaction region occurring at a supersonic compression corner when the wall-turning angle β_w is sufficiently large is shown in figure 1, together with a representative pressure distribution. In general terms the flow field can be considered as arising because the corner demands much too rapid a pressure rise. In inviscid flow a single shock would stand at the corner and turn the flow parallel to the downstream wall. In practice this shock wave intersects the boundary layer and the pressure rise is diffused upstream through the subsonic part of the boundary layer, causing it to thicken in advance of the corner. This thickening results in the supersonic part of the boundary layer being deflected outwards, which in turn causes compression waves to be generated in the boundary layer and propagated into the free stream. Evidently the upstream pressure distribution must be obtained by the growth of the boundary-layer displacement thickness, which, in fact, is governed by the very pressure distribution it is creating. This type of distribution has been termed self-induced and has been the subject of several studies (Honda 1958). Eventually a stage is reached where this self-induced pressure gradient becomes so large that the fluid at the surface cannot overcome it and so separates from the surface leaving a 'dead air' pocket underneath.

This separated layer of fluid entrains fluid from the dead-air region by the action of the shear stresses until it approaches the downstream wall. At this

point mass conservation requires all the entrained fluid to be reversed into the cavity. Evidently, the greater the length over which this entrainment takes place the higher the velocity on the streamline which must stagnate and so close the cavity (commonly called the dividing streamline). It also follows from this that, the greater the length from the separation point, the higher is the general level of velocity above this dividing streamline. Since the ability of a shear layer to re-attach and sustain the remainder of the pressure rise must be directly related to the general velocity level above the dividing streamline, it follows that to meet the demands for a larger turning angle the separation point moves upstream.

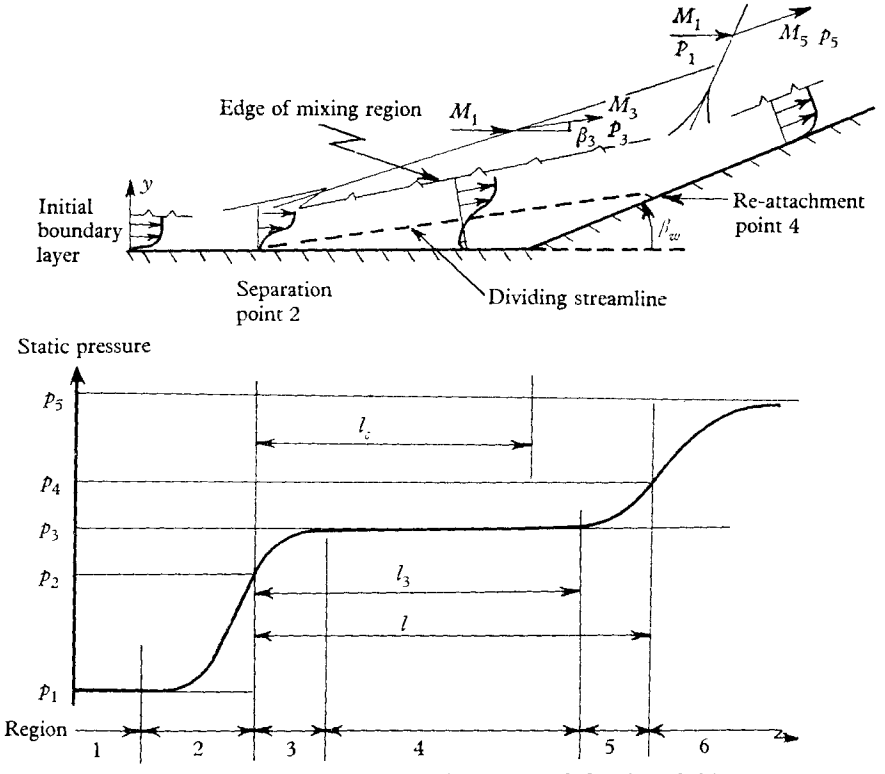

FIGURE 1. Diagrammatic sketch of the flow field.

Recently an attempt was made (Sanders & Crabtree 1963) to put the foregoing on a quantitative basis using the model of separated flow first introduced independently by Chapman, Kuehn & Larson (1959) and Korst, Chow & Zumwalt (1959). This attempt had little success due to the fact that, as pointed out by the authors, for simplicity a velocity profile was adopted which could not give the required variation of the velocity ratio on the dividing streamline. Cooke (1963), however, removed this objection by introducing the effect of the initial boundary layer on the shear-layer velocity profile and at the same time substituted a modified recompression criterion for the one proposed by Chapman and Korst. This previously adopted criterion was simply that the total pressure of the dividing streamline was equal to the static pressure at infinity. Cooke pointed out that in fact the total pressure of the stagnating streamline appeared

to be considerably less than this, and suggested that re-attachment occurred half-way up the pressure rise. Nash (1962*b*) was led to a similar conclusion but in some later unpublished work suggested that the re-attachment pressure rise varied quite substantially with both Mach number and Reynolds number. White (1963) has also utilized this modified recompression criterion in a very similar manner to Cooke (1963). In order to circumvent the problem of estimating this pressure rise to re-attachment coefficient N, McDonald (1964) placed the recompression criterion on a boundary-layer footing. In this note it was suggested that the pressure rise which occurs in practice is such that the velocity profile emerging from the recompression region is of the flat-plate type. Following from this an approximate method of calculating the final boundary-layer thickness parameters was advanced. Using this a limited analysis of some experimental results showed that the calculated profile shape parameter, that is the ratio of boundary-layer displacement to momentum thickness at the end of the pressure rise, was quite close to the estimated flat-plate value.

In the present note the analysis of McDonald (1964) is extended to take account of the finite length over which this re-attachment takes place. In view of the much more gradual pressure rise to re-attach the shear layer in the present circumstances, a two-layer model of the recompression process is substituted for the previously adopted one-layer model.

2. Method of solution

Study of the pressure distribution in figure 1 reveals the various regions into which the flow may be divided. In region 1 a uniform stream of external Mach number M_{e1} and static pressure p_1 approaches the corner. In region 2 this flow experiences a pressure rise until the boundary layer separates from the wall at a point where the external stream conditions are M_{e2} and p_2. From this point the pressure gradient decreases in region 3 to a plateau condition specified by M_{e3} and p_3. The flow in region 4 is considered to be at a constant pressure equal to this plateau value until the effect of the approaching wall is felt in region 5. This pressure rise characterises the recompression region where the fluid entrained in region 4 is reversed back to the cavity. The end of this region is marked by the re-attachment point where the static pressure is p_4 and the free stream Mach number M_{e4}. In region 6 this newly attached boundary layer is subjected to a further pressure rise until it reaches p_5 and M_{e5}, the overall value required by the corner.

These individual regions will now be dealt with in turn, the object being to trace the boundary-layer development from region 1 to region 6 and so specify the separation point by an iterative process based on the condition of the boundary layer emerging from region 6. A momentum-integral approach is adopted and a separation point is first of all assumed. The subsequent boundary-layer development in terms of the momentum thickness and shape parameter is then calculated. Depending on whether the calculated final shape parameter is greater than or less than the appropriate flat-plate value, the separation point is moved downstream or upstream.

At the start of each of the sections dealing with the analysis a brief outline of the subsequent treatment is given. Readers only interested in obtaining a general impression of the approach used can therefore omit the detailed analysis.

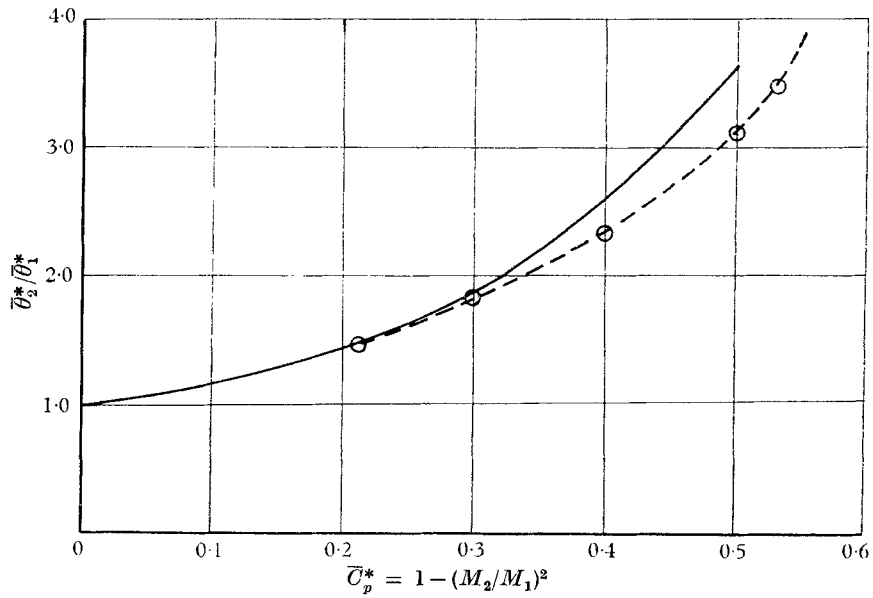

FIGURE 2. The boundary-layer momentum thickness at separation. ——, Predictions of Stratford (1959); – – ○ – –, predictions of Reshotko & Tucker (1955).

3. The boundary layer up to separation

In this section some of the currently available methods of predicting the boundary-layer momentum thickness at separation and the pressure rise to separation are briefly introduced. It is pointed out that the two simplest methods of predicting the momentum thickness at separation give very similar results. The problem of determining the shape parameter is avoided by assuming the velocity profile at separation to be similar to the asymptotic, free, half-jet profile.

Analysis

The problem of predicting the boundary-layer development under the influence of these largely self-induced pressure gradients has been of considerable interest to a number of investigators. Honda (1958) provides a method of solution which would give the boundary-layer and pressure distribution up to the separation point for a given starting point. In view of the difficulty, however, of obtaining the detail pressure distribution from the separation point to the plateau pressure (and from the plateau up to the re-attachment point) it has been decided to concentrate on predicting the overall scale of the interaction only, leaving the detail pressure distribution as a subject for future investigators. Having thus restricted the analysis the problem is therefore reduced to one of predicting the condition of the boundary layer at separation and the pressure rise to this point.

A particularly useful analysis of a separating incompressible turbulent boundary layer has been given by Stratford (1959). In this analysis Stratford gives a comparison between the theoretical and experimental variation of momentum thickness at separation with the pressure coefficient at this point. The momentum thickness at separation was non-dimensionalized by division by the momentum thickness of a comparison boundary layer. This comparison boundary layer was assumed to grow over the same horizontal distance but without the influence of the adverse pressure gradient. Good agreement between the theoretical predictions and the experimental measurements was obtained.

In order to utilize the foregoing incompressible solution the compressibility transformation of Mager (1959) is introduced. Basically this transformation specifies a co-ordinate transformation such that the compressible equations of motion are reduced to their incompressible equivalents.

However, this transformation has been the subject of some criticism recently, mainly on the question of the correct method of transforming the horizontal length scale. While this criticism is quite justified, in the present case the horizontal length is only of minor importance and so it is felt that this transformation will yield reasonable results. Thus, using the transformation, solutions valid in incompressible flow can be carried over to compressible flow. Under the transformation the following relationships are obtained

$$\theta = \bar{\theta}^*\{1 + \tfrac{1}{2}(\gamma - 1) M_e^2\}^3, \tag{1}$$

$$Cp_s = 1 - \left(\frac{\bar{u}^*_{e2}}{\bar{u}^*_{e1}}\right)^2 = 1 - \left(\frac{M_{e2}}{M_{e1}}\right)^2, \tag{2}$$

where θ is the boundary-layer momentum thickness and M_e is the local Mach number at the edge of the boundary layer. Cp_s is the incompressible pressure coefficient at separation and M_{e2}/M_{e1} is the ratio of the free-stream Mach number at separation to the initial free-stream Mach number. The bar and asterisk denote the incompressible quantity. On the assumption that the interaction length is short, the momentum thickness of Stratford's comparison boundary layer may be considered to be the same as the momentum thickness at the start of the interaction, that is θ_1. With this assumption and using (1) and (2), Stratford's relationship for the change in momentum thickness at an abrupt pressure rise is plotted in figure 2.

A somewhat different approach to this same problem has been developed by Reshotko & Tucker (1955) and uses the momentum and moment-of-momentum equations. This approach is discussed in Appendix 2 and only the results are mentioned here. First, the change in transformed shape parameter is given by

$$M_{e2}/M_{e1} = f(\bar{H}^*_2)/f(\bar{H}^*_1), \tag{3}$$

where

$$f(H) = \frac{H^2}{(H^2-1)^{\frac{1}{2}}(H+1)} \exp\left(\frac{1}{H+1}\right), \tag{4}$$

and secondly the change in momentum thickness is given by

$$\bar{\theta}^*_2/\bar{\theta}^*_1 = g(\bar{H}^*_2)/g(\bar{H}^*_1), \tag{5}$$

where

$$g(H) = \frac{(H^2-1)^{\frac{3}{2}}(H+1)}{H^4} \exp\left(-\frac{1}{H+1}\right). \tag{6}$$

Using (3)–(6) a plot of $\bar{\theta}_2^*/\bar{\theta}_1^*$ against Cp_s was obtained and is denoted by the circled points on figure 2. It can be seen that quite good agreement is obtained between this approach and the solution of Stratford, which, it should be remembered, compares very well with experiments at low speeds.

In a similar fashion to the plot of $\bar{\theta}_2^*/\bar{\theta}_1^*$ *vs* Cp_s Stratford gives a relationship between $\bar{H}_2^*$ and Cp_s. Later in the present analysis it becomes possible to simplify the evaluation of the free shear-layer profile (the velocity profile in region 4) if the velocity profile of the boundary layer at separation closely resembles the velocity profile of an asymptotic shear layer. Failing this, the simplification holds good if the initial boundary layer is small in comparison with the free shear-layer development length (see Nash 1962*a*). While in the present case this second reason might not be valid, it is a well-known fact that the velocity profile of a separation boundary layer closely resembles the asymptotic shear-layer profile when the pressure rise to separation is quite large. Adoption of this approximation makes any further investigation of the transformed shape parameter at separation unnecessary and in order to complete this aspect of the solution only the pressure rise to separation remains to be determined.

Several empirical, semi-empirical and theoretical methods are available to predict the pressure rise to separation, e.g. Chapman *et al.* (1959), Mager (1959), Reshotko & Tucker (1955). A very convenient theoretical relationship in good agreement with the experimental evidence is given by Ray (1962) as

$$\frac{p_2-p_1}{\gamma p_1 M_{e1}^2} = 0{\cdot}473\, C_h^{\frac{2}{3}} R_e^{-\frac{1}{10}} (M_{e1}^2-1)^{\frac{1}{4}} (1+M_{e1}^2/5)^{\frac{5}{8}} \tag{7}$$

(provided that separation does in fact occur; should separation not occur, in certain circumstances very much larger pressure rises than this can be sustained). In (7), C_h is the Chapman constant relating the viscosity to temperature,

$$\mu/\mu_w = C_h(T/T_w), \tag{8}$$

and for the present purposes a value of C_h of around 0·9 is suggested.

Thus using equation (7) the pressure rise to separation is obtained. Using either oblique shock or isentropic relationships (little difference arises from using either form) this pressure rise is converted to a Mach number change. This Mach number change may then be used to read off a value of $\bar{\theta}_2^*/\bar{\theta}_1^*$ directly from figure 2 or to evaluate a value from equations (3)–(6). This completes the information required at the separation point.

4. The pressure rise from separation to the plateau

Mager (1956) postulates that the pressure rise after separation is the result of the transverse pressure gradients and on this basis goes on to derive a simple relationship between the plateau pressure p_3 and the separation pressure p_2 given as

$$\frac{p_3}{p_2} = 1+0{\cdot}328\,\frac{\gamma M_{e2}^2 \beta_3}{1+\frac{1}{2}(\gamma-1)M_{e2}^2}, \tag{9}$$

where β_3 is the free-stream flow deflexion angle in the plateau region 4. It turns out that equation (9) is in good agreement with experiment but, as β_3 is not in

fact known *a priori*, the method involves an iteration with β_2, the free-stream flow deflexion angle at separation as the first approximation to β_3.

The next problem is to calculate the momentum thickness at the end of region 3. Unfortunately this is very difficult to achieve at the present time. In view, however, of the small magnitude of the pressure rise from separation to the plateau value (typically of the order of 5–10 % p_2) it is proposed to ignore the effect of this further pressure rise on the momentum thickness at separation and write

$$\bar{\theta}_2^* = \bar{\theta}_3^*. \tag{10}$$

This completes the development up to the start of region 4, the constant pressure plateau region.

5. The plateau region

In this region three problems are faced. The first is the prediction of the shear-layer velocity profile at any station downstream of the separation point. The second is the fixing of this velocity profile in space, and the third is concerned with relating the shear-layer velocity profile to the scale of the interaction.

The first problem is solved by adopting the approximate method of Kirk (1959), who suggested that this profile could be represented by a displaced asymptotic profile, that is, a profile obtained with zero initial boundary layer at some false upstream origin. The second problem, that of locating the velocity profile in space, is solved by following the procedure outlined by Korst *et al.* (1959). Thus the shear-layer profile and its location in space at any specified length from the separation point is determined. In particular the dividing streamline, which in turn specifies condition of the boundary layer at re-attachment, can now be found if the appropriate length scales are known. It is argued by McDonald (1964) and later in the present note that the appropriate length scales are l_3 and l (see figure 1) and an approximate method of calculating these length scales is advanced.

(*a*) *The velocity profile*

The problem of determining the shear-layer velocity profile is detailed fully by McDonald (1964) so only the main results are quoted here. It should be pointed out that using this approach the solution is restricted to zero heat transfer and a unit Prandtl number fluid. The velocity profile is given by

$$u^*/u_e^* = \phi = \tfrac{1}{2}(1+\operatorname{erf}\eta^*), \tag{11}$$

where

$$\eta^* = \frac{\sigma^* y^*}{X^*}, \quad \operatorname{erf}\eta^* = \frac{2}{\pi^{\frac{1}{2}}}\int_0^{\eta^*} \mathrm{e}^{-t^2}\,dt, \quad X^* = x^* + s^*. \tag{12}$$

In accordance with Kirk's approximation and using a value of the mixing coefficient $\sigma^* = 12$, it follows that

$$s^* = 30\bar{\theta}_3^*, \tag{13}$$

and the compressibility transformation is defined by

$$\psi^* = \psi, \quad x^* = x(1+\tfrac{1}{2}(\gamma-1)\,M_e^2)^{-1}, \quad y^* = \int_0^y \frac{\rho}{\rho_s}\,dy, \tag{14}$$

where ψ is the stream function, ρ_s is the stagnation density, that is, the density at the inner edge of the shear layer, and the asterisk denotes the transformed or incompressible quantity. It should perhaps be pointed out that the reason for using a transformation for the free shear layer other than the Mager transformation used earlier is that, in view of the fairly detailed experimental measurements available in this case, it has been found possible to obtain more accurate values (valid only for the free shear layer) for some of the free constants occurring in the transformation. Under the transformation the momentum thickness θ is transformed,

$$\theta^* = (\rho_e/\rho_s)\theta. \tag{15}$$

The integral I_1^* is defined as

$$I_1^*(\eta^*) = \int_{\eta^*}^{\eta_e^*} \phi \, d\eta^*, \tag{16}$$

and is plotted as a function of η^* in figure 5 of McDonald (1964) using a value of η_e^* corresponding to $\phi = 0{\cdot}999$. From these definitions and continuity it can be shown that the ordinate of the dividing streamline η_d^* is obtained from

$$\begin{aligned}\int_{\eta_d^*}^{\eta_m^*} \phi \, d\eta^* &= I_1^*(\eta_d^*) - I_1^*(\eta_m^*) \\ &= 12/[x/\theta_3\{1 + \tfrac{1}{2}(\gamma - 1)\, M_{ej}^2\}^{-2} + 30].\end{aligned} \tag{17}$$

This equation (17) can therefore be used to evalute η_d^* when the length x is known. From equation (11) η_d^* can be used to give ϕ_d, the velocity ratio on the dividing streamline. It remains to specify x and to do this the geometry of the problem must be introduced. It follows that the ordinates of certain streamlines which are known in the transformed plane will be required in the real plane. To do this use is made of the inverse transformation to equation (14), that is

$$y = \int_0^{y^*} \frac{\rho_s}{\rho} dy^*. \tag{18}$$

Noting that, for constant pressure, unit Prandtl number, and zero heat transfer

$$\rho_s/\rho = (1 - c^2\phi^2), \tag{19}$$

where c is the Crocco number defined by

$$c^2 = \tfrac{1}{2}(\gamma - 1)\, M_{e3}^2/[1 + \tfrac{1}{2}(\gamma - 1)\, M_{e3}^2], \tag{20}$$

the result obtained is

$$y = \frac{X^*}{\sigma^*} \int_0^{\eta^*} (1 - c^2\phi^2)\, d\eta^*. \tag{21}$$

It should be noted that the origin for the integration should be taken on the dividing streamline to be strictly in accordance with the transformation. In the region below $\phi = 0{\cdot}5$, however, and with c small, the contribution of the $c^2\phi^2$ term is very small. Furthermore, the real ordinate is not required to a high degree of accuracy so, in the inner region of the shear layer, it would appear sufficiently accurate to write

$$y = y^*. \tag{22}$$

Thus, a complete description of the shear-layer profile may be obtained provided the length of the plateau region x is known. The problem of determining this

length x (subsequently termed l_3) is studied in the following section. First of all the free shear layer is located with respect to the wall in (*b*). This is followed in (*c*) by a brief consideration of the geometry and an expression is derived for the length up to the hypothetical impingement point of any ordinate in the shear layer.

(*b*) *The axis shift*

In solving the partial differential equation of the free shear layer to yield equation (11), use is made of an intrinsic system of co-ordinates. In the present problem it is desired to relate this intrinsic system to some reference system of co-ordinates so that the geometry of the problem may be properly introduced. The relationship between the two co-ordinate systems is obtained by ensuring that the momentum equation is satisfied with respect to the reference system (the momentum equation is automatically satisfied referred to the intrinsic system). The reference system of co-ordinates is defined to represent the boundary of the corresponding inviscid jet (see figure 3). This inviscid jet is considered to be the

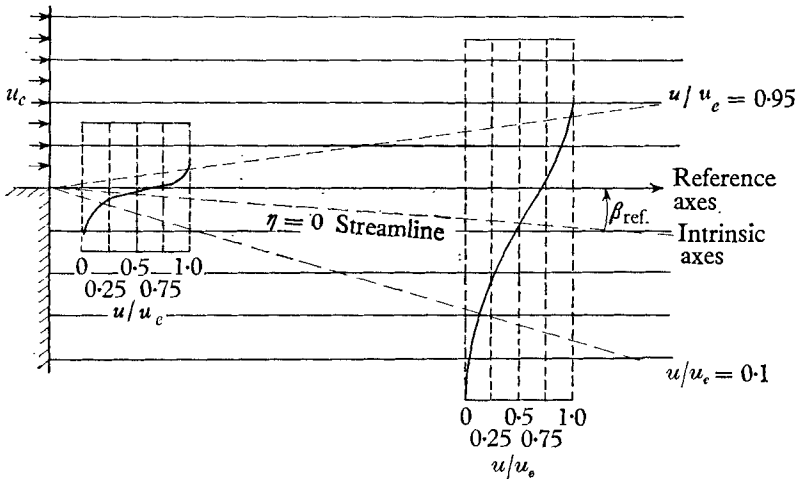

FIGURE 3. Spread of mean velocity in a two-dimensional half-jet after Liepmann & Laufer (1947).

path the fluid would take under the influence of identical external forces in the absence of the shear stresses. By defining the reference system in this fashion it is ensured that the two systems coincide at $x = 0$. Korst *et al.* (1959) give this origin shift and after some manipulation it can be put in the form

$$y_b = y_{\text{ref}} - \int_{-\infty}^{y_{\text{ref}}} \frac{\rho u^2}{\rho_e u_e^2} dy - [\Delta + \theta]_{x=0}, \tag{23}$$

where y_{ref} is a point sufficiently large such that $\phi \sim 1{\cdot}0$, y_b is the origin shift, and Δ and θ are the displacement and momentum thicknesses of the boundary layer at separation. Having already found Kirk's approximate representation of the mixing profile very useful it is natural to extend it to the present problem of determining the axis shift. Setting the initial boundary layer as zero at some

hypothetical upstream origin, applying the transformation and introducing the similarity parameter for the asymptotic free jet give

$$\frac{\sigma^* y_b}{X^*} = \eta^*_{\text{ref}} - \int_{-\infty}^{\eta^*_{\text{ref}}} \phi^2 d\eta^* + c^2 \int_{-\infty}^{0} \phi^2 d\eta^*. \tag{24}$$

Evaluating (24) using the tabulated error-function profile relationships given by Korst, Page & Childs (1955) gives

$$y_b = (X^*/\sigma^*)\,(0{\cdot}3989 + 0{\cdot}0826c^2),$$

where y_b is the shift between $\phi = 0{\cdot}5$ and the reference system passing through the virtual origin of the asymptotic shear layer (note that the asymptotic error-function ordinate origin is at $\phi = 0{\cdot}5$). Interpreting this shift as an angular deviation, β_{ref}, gives

$$\beta_{\text{ref}} = y_b/(x+s) = (0{\cdot}033 + 0{\cdot}0069c^2)\,(1-c^2), \tag{25}$$

and (25) gives the angular deviation between the two systems of axes β_{ref} as about 2° in incompressible flow and about 1° at $M = 2{\cdot}0$. Evidently the axis angular deflexion is a very small quantity which, although included in the subsequent analysis, can be safely neglected in most circumstances.

(*c*) *Geometrical aspects*

To obtain a solution to the present problem the length of the free shear has to be estimated. To do this curvature of the streamlines in the vicinity of the re-attachment point is neglected (see figure 5). If β is the angle between the ordinate of interest η and the shear-layer intrinsic axis, and h is the height from the wall to the ordinate of interest at the separation point then, from the geometry of triangle ABC in figure 4,

$$\frac{x+\delta l_1}{l_c+\delta l_2} = \frac{\sin\beta_w}{\sin[\beta_w - (\beta_3+\beta-\beta_{\text{ref}})]}, \tag{26}$$

where

$$\delta l_1 = \frac{h\cos(\beta_3-\beta_{\text{ref}})}{\sin(\beta_3-\beta_{\text{ref}}+\beta)}, \quad \delta l_2 = \frac{h\cos\beta}{\sin(\beta_3-\beta_{\text{ref}}+\beta)}, \tag{27}$$

and by definition

$$\beta = \frac{y}{x+s}, \quad h = 2{\cdot}5\theta^*_3 \int_{-1{\cdot}0}^{\eta^*} (1-c^2\phi^2)\,d\eta^*, \tag{28}$$

where it has been assumed that the inner edge of the shear layer is at $\eta^* = -1{\cdot}0$. Since the integral in (28) can be evaluated with the help of tabulated values (Korst *et al.* 1955) the problem is now one of determining the ordinate of interest. The first length of interest is the length up to the start of the pressure rise, l_3, and following McDonald (1964) this is assumed to occur when the ordinate at the inner edge of the shear layer y_i meets the fluid being reversed from the re-attachment region (see figure 5). Assuming that $y_i = y_i^*$ this results in

$$\beta = -2{\cdot}0/\sigma^*(1 + \tfrac{1}{2}(\gamma-1)\,M^2_{e3}) \tag{29}$$

and $h = 0$, so equation (26) can be solved for l_3. The problem of determining the ordinate of the dividing streamline so that the length l can be found is treated in §6.

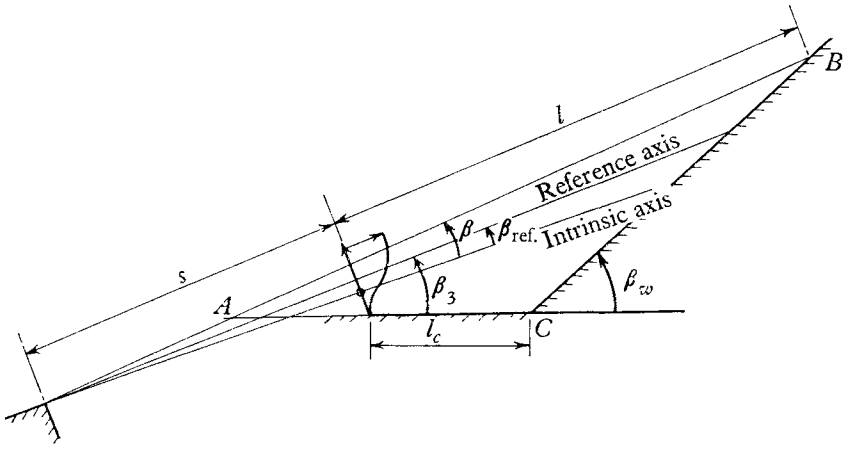

FIGURE 4. Sketch showing the flow geometry.

6. The velocity profile at re-attachment

In this section a two-layer model of re-attachment is suggested, after the manner of Stratford (1959). Here re-attachment is considered to be fairly abrupt, so that along streamlines of the mean flow in the outer part of the boundary layer isentropic recompression can be assumed. In the inner layer, however, the effect of the pressure gradient is countered by the shear gradient. Following from this, the velocity profile at the re-attachment point is specified in terms of the velocity ratio on the dividing streamline and the pressure gradient at re-attachment. A fairly simple approximate value of the re-attachment pressure gradient is suggested (see figure 5) and the profile thickness parameters and pressure rise at this point evaluated and presented graphically as a function of the velocity ratio on the dividing streamline. The problem now becomes one of finding the velocity ratio on the dividing streamline, and this is in part an iterative procedure. Conservation of cavity mass flow at the start of the pressure rise specifies the mass flow to be returned to the cavity. Downstream of the initial pressure rise and up to the re-attachment point the profile is assumed to continue to develop as a free shear layer. The velocity ratio on the dividing streamline is then obtained by locating the point in the shear layer at re-attachment which could reverse this required mass flow. The iteration occurs when it is remembered that the estimate of the length up to the re-attachment point requires a knowledge of the ordinate of the dividing streamline. To start the iteration the length up to the start of the pressure rise can be used.

Analysis

In general the difference between the overall corner-turning angle, β_w, and the flow-deflexion angle in the constant pressure region β_3 is not very great. Consequently the length over which re-attachment takes place is quite large and of the order of the length over which the shear layer develops. The problem therefore requires a knowledge of the effect of the wall shear stress, boundary-layer growth and pressure rise during the process of re-attachment. A sophisticated solution

to this problem, is, of course, out of the question at the moment. In order to proceed, the boundary layer is divided into an inner and outer layer after the fashion of Stratford (1959) and later improved by Townsend (1960, 1962).

In the outer layer the pressure rise is considered to be sufficiently abrupt as to make the shear stress contribution to the change in velocity a relatively minor one. In the inner layer the situation is completely reversed and here the pressure forces must be balanced by the gradient of the shear stress when the velocity approaches zero. The analysis of this section is developed entirely for incompressible flow on the assumption that to obtain the appropriate compressible result the transformation of Mager (1959) can be used. It follows from this that the symbols should all have a bar and asterisk superimposed, but for clarity of presentation this has been omitted save when the final results are presented in graphical form.

The x-equation of motion of an incompressible turbulent boundary layer can be written as

$$\frac{\partial}{\partial x}(p+\tfrac{1}{2}\rho u^2) = \frac{\partial \tau}{\partial y}, \tag{30}$$

along a streamline of the mean flow. With an abrupt pressure rise the major effect on the outer-layer velocity profile stems from the $\partial p/\partial x$ term and in fact Townsend (1960, 1962) ignored the $\partial \tau/\partial y$ contribution altogether in this outer region. Stratford (1959), however, introduced the concept of a 'comparison boundary layer' to estimate the effect of these Reynolds stresses in the outer region. Effectively this is equivalent to assuming that the Reynolds stresses along a given streamline in the outer layer remain constant at their initial value during the pressure rise. According to this suggestion, along a streamline in the outer layer (in incompressible flow)

$$(\tfrac{1}{2}\rho u^2)_4 = (\tfrac{1}{2}\rho u'^2)_3 - (p_4 - p_3), \tag{31}$$

where p_4 and p_3 are the static pressures (assumed constant in the y-direction) at the re-attachment point and the start of the pressure rise respectively. The prime denotes the comparison profile, the profile which would be developed if the pressure had remained constant between these two stations. This relationship gives the velocity profile in the outer layer and obviously can very readily be extended to the compressible case without the aid of the transformation. This is, in fact, what McDonald (1964) has done.

Considering now the inner layer, Stratford (1959) showed that, for y small and $\frac{1}{2}\rho u^2 \approx 0$, integration of (48) gives

$$\tau = \tau_d + y(dp/dx). \tag{32}$$

Using either dimensional analysis or mixing-length theory Stratford was able to show that when τ_d was zero (at re-attachment or separation) the velocity profile in the inner layer has the form

$$\tfrac{1}{2}\rho u^2 = \frac{2}{K_0^2}\frac{dp}{dx}y, \tag{33}$$

where K_0 is an absolute constant (subsequently taken as 0·40). Equations (31) and (33) give the velocity profile at re-attachment and it remains to join the two

solutions. Townsend pointed out that the join is specified by continuity of velocity, shear stress and mass flux. Continuity of velocity requires

$$\tfrac{1}{2}\rho u_j'^2 - (p_4 - p_3) = \frac{2}{K_0^2}\frac{dp}{dx} y_j, \tag{34}$$

where the subscript 'j' denotes the joining streamline.

On the assumption that the shear stress in the outer region can be determined from the concept of eddy kinematic viscosity, ϵ, independent of y there results

$$\tau_j = \tau_j' = \left(\rho\epsilon \frac{\partial u}{\partial y}\right)_j' = y_j \frac{dp}{dx}. \tag{35}$$

Continuity of mass flux gives

$$\int_0^y \rho u'\, dy' = \tfrac{2}{3}\rho \left(\frac{4}{\rho k_0^2}\frac{dp}{dx}\right)^{\frac{1}{2}} y_j^{\frac{3}{2}}. \tag{36}$$

Evidently if the velocity and shear stress distribution of the comparison profile are known then (34), (35) and (36) give a zero wall stress condition as a function of C_p and dC_p/dx where $C_p = (p_4 - p_3)/\frac{1}{2}\rho u_{e3}^2$. In the case of a separating boundary layer the potential flow pressure distribution can, in most cases, be used so that these three equations may be solved to predict the location of the separation point. However, in the case of a re-attaching boundary layer the potential flow (if it can be called such) is too closely linked to the viscous problem to be of much help. For example, before the potential flow solution can be made to bear any resemblance to the actual flow, the geometry of the separated flow region, itself a function of the base pressure, must be known (Nash 1964). Hence if any progress is to be made some assumption must be made regarding the pressure gradient at re-attachment. Having done this the three equations could then be solved for the pressure at the re-attachment point. This is done in rather a crude fashion as follows: from figure 5 it can be seen that, based on the earlier-mentioned hypothesis concerning the start of the pressure rise (§ 5 (*c*)), the length over which re-attachment takes place is given by

$$\delta x = 2(\beta_T - \beta)^{-1} y_i, \tag{37}$$

where

$$y_i = (y_d - y_{\phi=0})_{x=l_3}, \tag{38}$$

and similarly

$$\delta C_p = C_p. \tag{39}$$

Thus the pressure gradient is given approximately by

$$\frac{dC_p}{dx} = C_p \frac{(\beta_T - \beta)}{2y_i}. \tag{40}$$

Using this expression, (34), (35) and (36) are put in the form

$$\phi_j'^2 = \left[16(\tau_j/\rho u_{e3}^2)^{\frac{3}{2}} y_i \Big/ 3K_0(\beta_T - \beta)\int_{y_d'}^{y_j'} \phi'\, dy'\right] + \frac{2}{K_0^2}(\tau_j/\tfrac{1}{2}\rho u_{e3}^2), \tag{41}$$

$$C_p = \phi_j'^2 - (2/K_0^2)(\tau_j/\tfrac{1}{2}\rho u_{e3}^2), \tag{42}$$

$$y_j = \frac{K_0^2(\phi_j'^2 - C_p)\, y_i}{C_p(\beta_T - \beta)}, \tag{43}$$

and from these equations the pressure rise to re-attachment and the velocity profile at re-attachment may be determined. It is noted that this set of equations would have to be solved for each particular geometry involved, so obviously further simplification is desirable. This is achieved by noting that, to the same degree of approximation as was adopted in estimating the pressure gradient,

$$y_i = y_i' \tag{44}$$

and

$$\beta_T - \beta = \text{const.} = 0{\cdot}25. \tag{45}$$

The first approximation may be justified by noting that as the inner edge of the comparison boundary layer grows so the ordinate of the dividing streamline

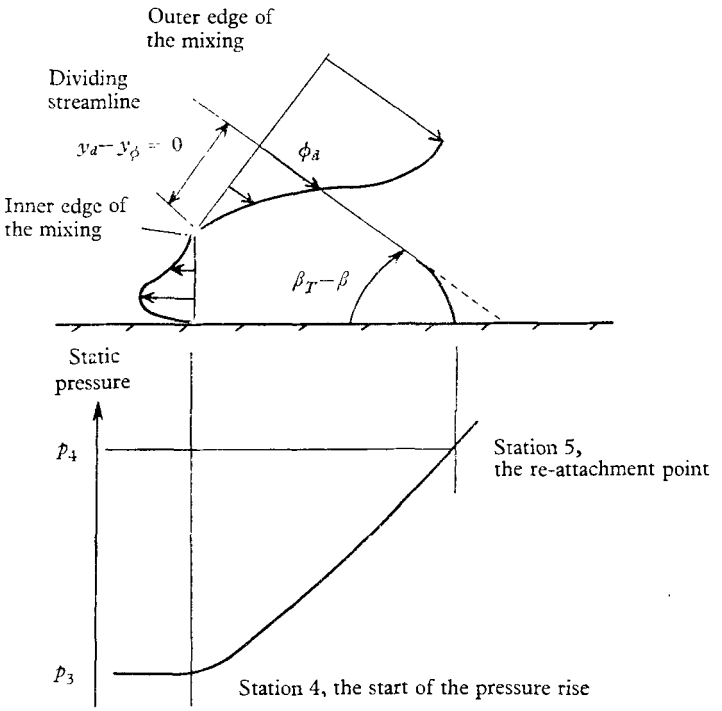

FIGURE 5. Sketch of the re-attachment region.

decreases, a move dictated by the requirement to return a fixed mass flow upon re-attachment. The second of these approximations is known to be quite accurate, especially when β is small (Love 1957). In order to obtain a generalized solution it is now only necessary to adopt a velocity profile and put values to numerical constants. In view of the difficulty involved in using the error-function profile introduced earlier, the easily integrated and very similar sine profile was adopted, that is

$$\phi = \tfrac{1}{2}(1 + \sin \eta^*), \tag{46}$$

together with, of course, Kirk's approximation. Taking $K_0 = 0{\cdot}40, \sigma^* = 12$ and $\eta_{\phi=0} = -1{\cdot}0$, C_p was calculated as a function of ϕ_d' by an iterative process. This is plotted in figure 6 and here a direct comparison can be made between the two-layer model adopted here and the one-layer model used previously. In the

latter case C_p is simply equal to $\phi_d'^2$ under the assumption of isentropic recompression of the dividing streamline. It is apparent from figure 6 that, in view of the cross-over obtained on comparing these two approaches, some error of cancellation must have been present in the one-layer model and probably arose because the loss in total head due to Reynolds stress is balanced by the increase in pressure rise possible because of the profile at the wall distorting to give zero wall shear stress. This result probably explains the success of methods such as those used by McDonald (1964), where isentropic recompression has been assumed. The analysis is now continued to enable the various thickness parameters of the profile at the re-attachment point to be determined.

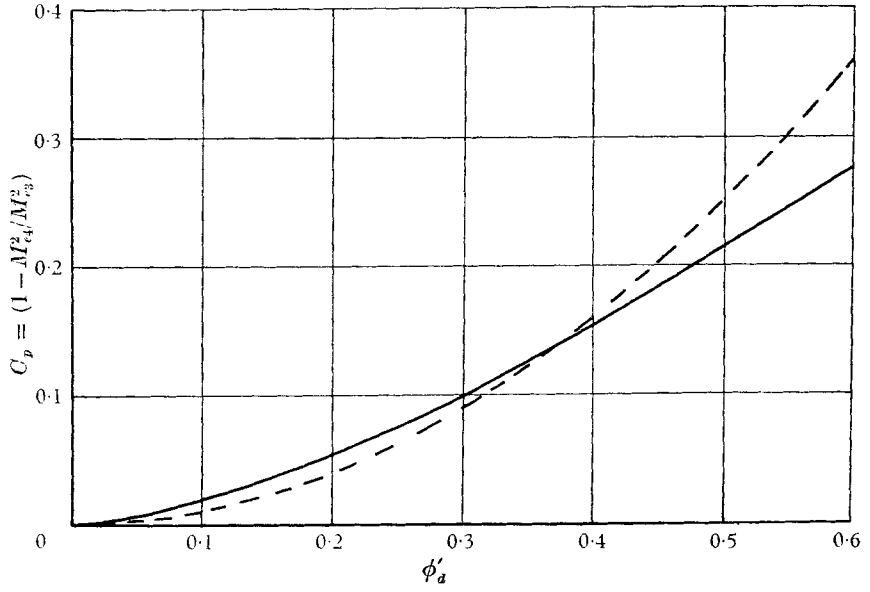

FIGURE 6. The pressure rise to re-attach the shear layer as a function of the velocity ratio on the dividing streamline. ——, Two-layer theory; – – –, one-layer theory. McDonald (1964) ($C_p = \phi_d'^2$).

From continuity considerations the boundary-layer thickness at re-attachment δ_4 is given by

$$\delta_4 = \frac{3}{2}\int_{y_d'}^{y_e'} \phi' d\eta' \left[\frac{2}{K_0^2}\cdot\frac{\tau_i}{\frac{1}{2}\rho u_{e3}^2}\right]^{-1} + \int_{y_j'}^{y_e'} \frac{\phi'}{(\phi'^2 - C_p)^{\frac{1}{2}}}\, dy'. \tag{47}$$

From the definition of displacement thickness and the known profile at re-attachment the boundary-layer displacement thickness at the re-attachment point, Δ_4, is given by

$$\Delta_4 = \delta_4 - \frac{1}{(1-C_p)^{\frac{1}{2}}}\left[\tfrac{2}{3} y_j \left(\frac{2}{K_0^2}\frac{\tau_j}{\frac{1}{2}\rho u_{e3}^2}\right) + \int_{y_j'}^{\delta'} \phi'\, dy'\right], \tag{48}$$

and similarly the momentum thickness at re-attachment θ_4 is given by

$$\theta_4 = \delta_4 - \Delta_4 - \frac{1}{(1-C_p)}\left[\frac{y_i}{K_0^2}\left(\frac{\tau_j}{\frac{1}{2}\rho u_{e3}^2}\right) + \int_{y_j'}^{\delta'} \phi'(\phi'^2 - C_p)^{\frac{1}{2}} dy'\right]. \tag{49}$$

These expressions have been evaluated using the sine profile and are given graphically in figures 7, 8 and 9. In Appendix 1 the appropriate transformation relationships are given so that the foregoing analysis can be used to predict the change in compressible boundary-layer parameters. In order to complete this estimate of the boundary layer at re-attachment it remains to determine ϕ'_d, the velocity ratio of the dividing streamline of the comparison profile. This is done in the subsequent section.

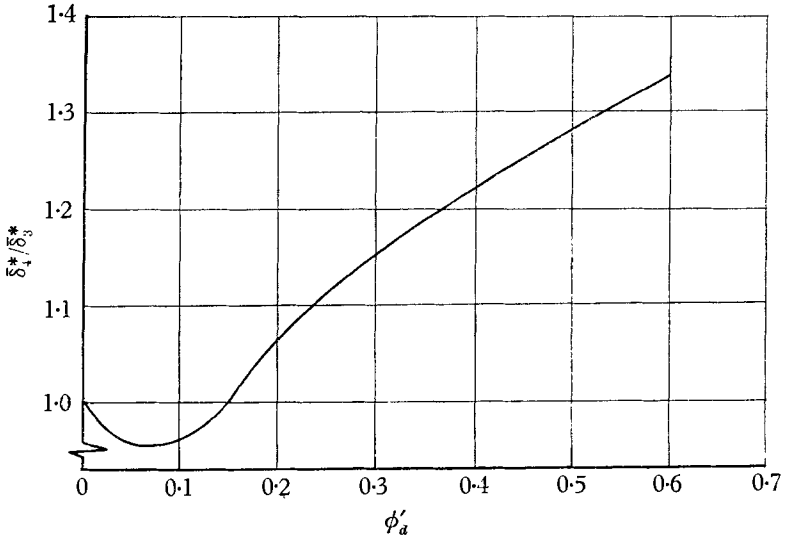

FIGURE 7. The boundary-layer thickness at the re-attachment point. $\bar{\delta}_3^*$ $\bar{\delta}_4^*$, transformed profile thickness above the dividing streamline at the start of the pressure rise and at the re-attachment point, respectively.

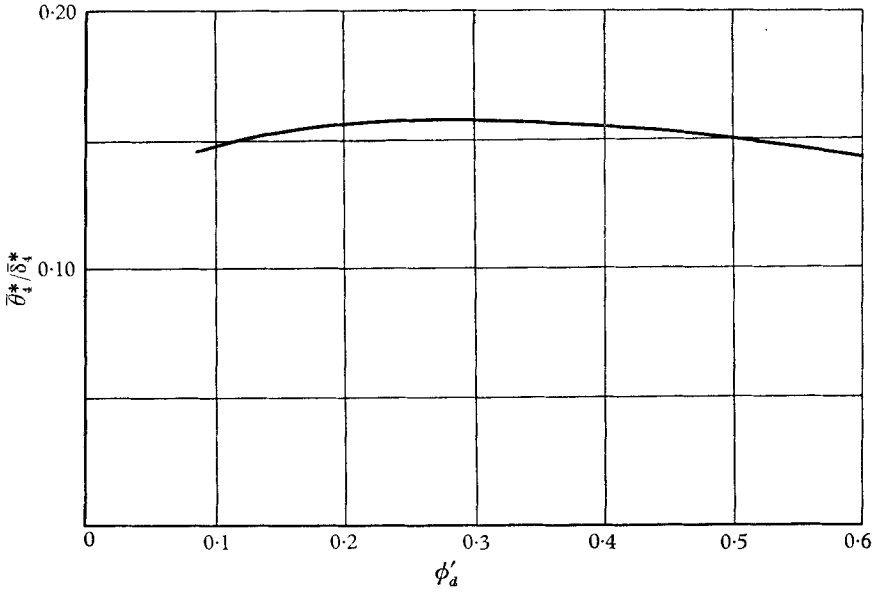

FIGURE 8. The boundary-layer momentum thickness at the re-attachment point.

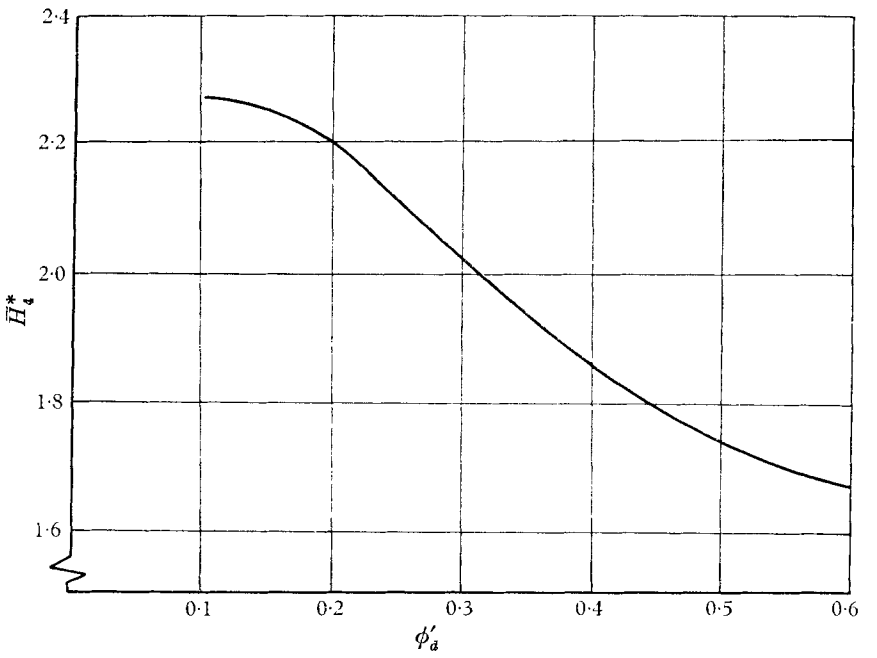

FIGURE 9. The boundary-layer shape parameter at re-attachment.

The comparison profile

The velocity ratio on the dividing streamline of the comparison profile is obtained by remembering that the mass flow to be returned to the cavity is given by

$$\frac{m_{\text{rev}}}{\rho_s u_{e3}} = \frac{L_3^*}{\sigma^*}\int_{-\infty}^{\eta_m^*} \phi\, d\eta^* - \theta_3^*, \tag{50}$$

where

$$L^* = l\{1 + \tfrac{1}{2}(\gamma - 1)\, M_{e3}^2\}^{-1} + 30\theta_3^*.$$

This mass flow is equated to the mass flow in the shear layer below η_d^* at length l from separation, that is

$$\frac{m_{\text{rev}}}{\rho_s u_{e3}} = \frac{L^*}{\sigma^*}\left[\int_{-\infty}^{\eta_m^*} \phi\, d\eta^* - \int_{\eta_d^*}^{\eta_m^*} \phi\, d\eta^*\right],$$

which gives

$$I_1^*(\eta_d^*) = \left(1 - \frac{L_3^*}{L^*}\right)\int_{-\infty}^{\eta_m^*} \phi\, d\eta^* + I_1^*(\eta_m^*) + \frac{\sigma^*\theta_3^*}{L^*}. \tag{51}$$

Using a value of $\int_{-\infty}^{\eta_m^*} \phi\, d\eta^*$ of 0·3989, obtained from Korst *et al.* (1955) this equation can be solved to give η_d^*, and so ϕ_d' is obtained once the length l is determined. Since it has been demonstrated earlier in §5(*c*) that l is in fact determined by η_d^*, an iterative process is indicated here.

7. The re-adjustment region

In this section the flow downstream of re-attachment and up to the end of the pressure rise is considered. It is pointed out that the treatment of this part of the flow development given by McDonald (1964) can be expected to hold in the present circumstances. For this reason the method of McDonald, which in essence is based on the Squire & Young formula (1937), is utilized to predict the boundary-layer condition at the end of the pressure rise specified by the corner. This is compared with the corresponding flat-plate profile shape parameter and the separation point moved either upstream or downstream depending on whether the estimated shape parameter is less than or greater than the corresponding flat-plate value.

Analysis

McDonald (1964) has shown that the boundary layer downstream of re-attachment should be estimated using a method based on the semi-empirical formula of Squire & Young (1937). However, as this formula represents a wake recompression law, the calculation required the wall shear stress to be negligible during the recompression process. In the cases to which this was applied there was little doubt that this condition was satisfied. This, however, may no longer be true as in the present analysis the length over which the layer readjusts is quite large. In Appendix 2 this point is considered in some detail and it is shown that even in the present instance it is still a reasonable assumption to neglect the effect of the wall shear stress on the thickness parameters.

In view of this the solution to this aspect of the problem given by McDonald (1964) is utilized. This gives the appropriate changes as

$$M_{e5}/M_{e4} = f(\bar{H}_4^*)/f(\bar{H}_5^*), \tag{52}$$

where $f(\bar{H}^*)$ is defined by (4), $\bar{H}^*$ by (A 1.3), M_{e4} is given by

$$C_p = 1-(M_{e4}/M_{e3})^2, \tag{53}$$

and M_{e5} given by the overall corner-turning angle and the isentropic flow tables. The change in momentum thickness is obtained from

$$\bar{\theta}_5^*/\bar{\theta}_4^* = g(\bar{H}_4^*)/(g(\bar{H}_5^*), \tag{54}$$

where $g(\bar{H}^*)$ is defined by (6).

Thus using equations (52) and (54) an approximate evaluation of the boundary-layer thickness parameters at the end of the pressure rise can be made. Following McDonald (1964) the hypothesis is advanced that this final profile must be of the flat-plate type and as such can be specified by the shape parameter given by

$$\bar{H}^* = 1{\cdot}754 - 0{\cdot}149\log_{10}\bar{R}_{\theta*}^* + 0{\cdot}01015[\log_{10}\bar{R}_{\theta*}^*]^2, \tag{55}$$

which is Maskell's curve fit (1951) to the experimental flat-plate data of Ludwieg & Tillman (1950) transformed to compressible flow using Mager (1959). In the above the Reynolds number transformation is given by

$$\bar{R}_{\theta*}^* = \{1+\tfrac{1}{2}(\gamma-1)M_e^2\}^{-0{\cdot}76}R_\theta. \tag{56}$$

Using the above an iteration is thus set up for the separation point.

8. A summary of the development

In view of the length of the calculation it is thought worthwhile to detail the development as a series of steps. Given the overall corner angle β_w, the initial Mach number M_{e1}, and the boundary-layer momentum thickness upstream of the corner, θ_1, a separation location, l_c, is chosen and the procedure is as follows:

(i) From (7) estimate p_2 and hence M_{e2} and β_2, following with an iteration using (9) to obtain p_3, M_{e3} and β_3.

(ii) Using (3)–(6) (or figure 2) obtain $\theta_2 (\sim \theta_3)$.

(iii) From (25) find β_{ref}, from (29) find β and so from (26) locate l_3.

(iv) With $l = l_3$ solve (51) to give a first approximation to η_d^*. Return to (28) and so estimate β and h using (21) or (22) and Korst *et al.* (1955). These are used in (26) to obtain a second approximation to l. Using this value, (51) gives a second approximation to η_d^*, which from (11) gives ϕ_d'. Probably only one iteration will be required.

(v) From figures 6–9 the values of C_p, $\bar{\delta}_4^*/\bar{\delta}_3^*$, $\bar{\theta}_4^*/\bar{\delta}_4^*$ and $\bar{H}_4^*$ are obtained. From C_p, M_{e4} is obtained via (53).

(vi) From either shock-wave tables or tables of isentropic flow M_{e5} is calculated. Thus using (52) and (4), $\bar{H}_5^*$ is calculated. Using (54) and (6) $\bar{\theta}_5^*$ is then estimated.

(vii) Using (55) and (56), $\bar{H}^*$ flat plate is calculated and compared with $\bar{H}_5^*$. If $\bar{H}_5^*$ is larger than $\bar{H}^*$ flat plate the separation point is moved downstream and vice versa if $\bar{H}_5^*$ is smaller than $\bar{H}^*$ flat plate.

9. A comparison with experiment

To check the accuracy of the foregoing analysis the inviscid shock configuration existing at a corner was adopted and the final shape parameter calculated. This was done for pressure distributions given by Chapman *et al.* (1959) where the free-stream Mach number was 2·7. The results are given in figure 10, where it can immediately be seen that the calculated value of the final shape parameter agrees quite closely with the corresponding flat-plate value. As a test of the suitability of this procedure for the calculation of the shock configuration the separation point in one case was moved upstream and the length l_c doubled. This resulted in about a 50 % increase in the value of the calculated final shape parameter so on this basis it is thought that the proposed method would be sufficiently sensitive.

Further to this calculation the shape parameter was evaluated by the method of McDonald (1964) for the pressure distributions of Chapman *et al.* (1959) and it can be seen from figure 10 that, doubtless by a process of error cancellation, not much difference exists between the two calculations.

Recently a detailed experimental investigation of this type of corner flow has been reported by White (1963). Unfortunately in this case the upstream boundary layer was forced to separate from a circular cylinder so the pressure rise to a separation and the plateau pressure ratio could not be estimated using the relationships given in this note. However, it is felt that these relationships have been adequately verified elsewhere. In order to use these results as a test of the present method the experimental separation point was adopted and the

pressure rise across the second shock calculated. In figure 11 this is shown to be in fairly good agreement with the measured pressure rise. To relate this agreement in pressures to the scale of the interaction it should be noted that 0·1 in pressure ratio would alter the shear layer length by about 25 %.

A rather interesting confirmation of the present two-layer analysis is to be found in the experimental work of Nash *et al.* (1963) and in the work of White (1963). In these references the re-attachment conditions of a compressible shear

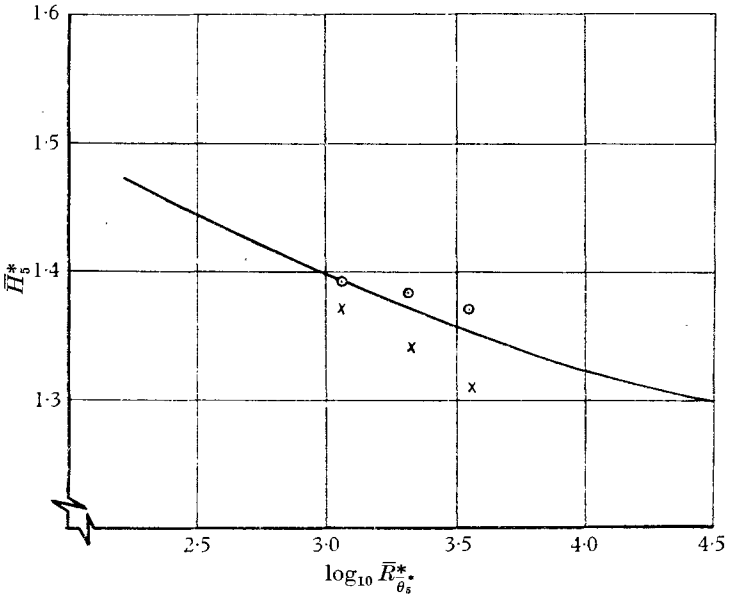

FIGURE 10. The shape parameter at the end of the pressure rise. ⊙, Chapman *et al.* (1959), calculated value according to two-layer analysis of present note for the experimental results. —, Ludweig & Tillman flat-plate shape parameter (1950). ×, One-layer model applied to Chapman *et al.*'s (1959) experimental results.

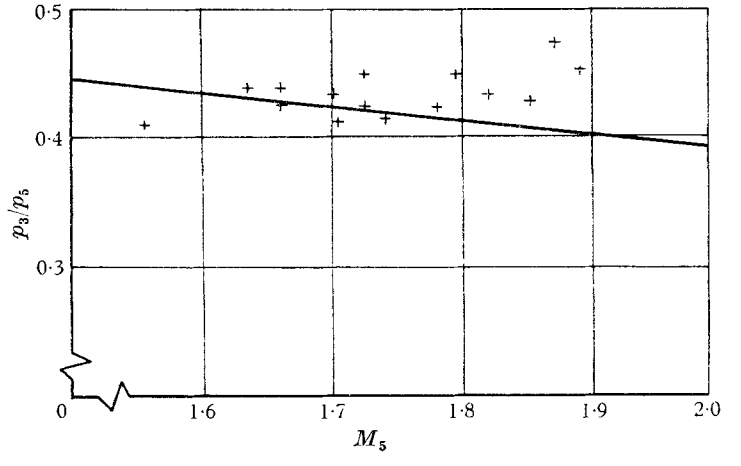

FIGURE 11. A comparison between measured and estimated plateau pressures. +, Experiments of White (1963). ——, Estimate of present note.

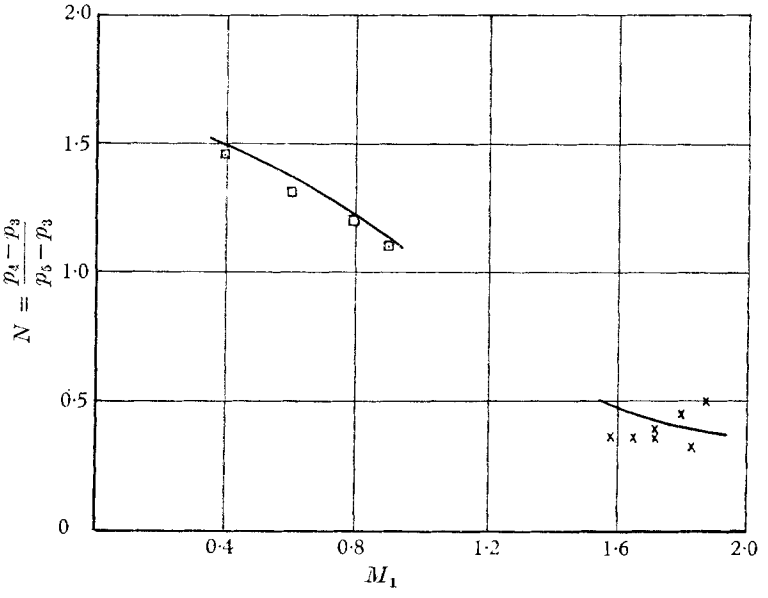

FIGURE 12. A comparison between measured and predicted pressure rise required to re-attach the shear layer. ⊡, Nash (1963); ×, White (1963), measured re-attachment pressure rise coefficient. ——, Calculated value from present analysis.

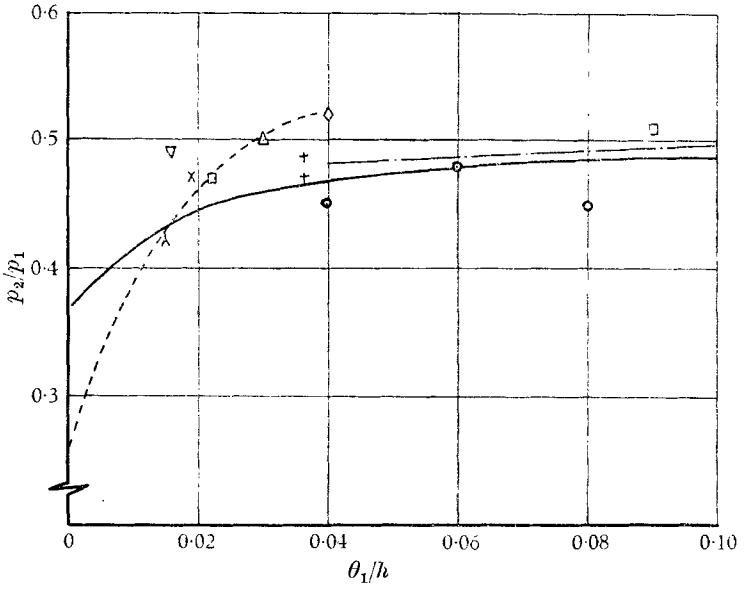

FIGURE 13. A comparison between measured and predicted base pressure at $M = 1{\cdot}5$. Experiments of: △, Beastall & Eggink (1951); ⊡, Hastings (1963); ×, Sirieux (1960); λ, Gadd *et al.* (1955); —·—, Chapman *et al.* (1952); ◇, Wimbrow (1954); +, Morrow & Katz (1955); ⊙, Goin (1952); ▽, Saltzman (1961). ——, Present note, $-R_{\theta_1} = 10^4$; – – – –, method of McDonald (1964), $H_5^* = 1{\cdot}4$.

layer were measured and expressed in terms of a recompression parameter N, given by

$$N = (Cp_r - Cp_b)/(-Cp_b), \tag{57}$$

where

$$Cp_r = (p_4 - p_1)/\tfrac{1}{2}\rho u_{e1}^2, \quad Cp_b = (p_3 - p_1)/\tfrac{1}{2}\rho u_{e1}^2. \tag{58}$$

From the quoted base pressures and the measured N values it is a simple matter to compute Cp, that is, $1-(M_{e4}/M_{e3})^2$. Using the experimental lengths of shear-layer development (a necessity in this case since the results of Nash 1963 are subsonic) together with the measured initial boundary layer an estimate of the velocity ratio on the dividing streamline was made. From figure 6 a theoretical value of Cp was then obtained and this is compared with the measured values in figure 12, and it is evident from this that a fair degree of agreement has been obtained. Finally it is worth noting that the present two-layer analysis can be used to extend the range of initial boundary-layer thickness for which the analysis of McDonald (1964) is valid. The method of doing this is simply to follow McDonald's analysis as outlined until it is desired to calculate the profile at re-attachment. This part is analysed according to the present note and the subsequent development calculated according to McDonald. In figure 13 the results of some base pressure calculations according to this method are compared both with experiment and the method of McDonald (1964). It can be seen that a considerable degree of agreement with experiment has been obtained.

10. Conclusions

It would appear that the base pressure analysis given by McDonald (1964) is capable of being developed and that a fairly accurate estimate of the inviscid shock position occurring at a large-angle compression corner can be made. In obtaining this solution, however, we have introduced many additional assumptions whose validity must be tested by further more detailed experiments. These additional assumptions are now summarized:

1. The effect of the pressure rise from the separation point to the plateau pressure has a negligible effect on the boundary-layer momentum thickness.
2. The velocity profile at the start of the plateau region is adequately described by Kirk's approximation (1959).
3. The pressure gradient at re-attachment is given approximately by the relationship suggested, and is sufficiently large for a two-layer model of re-attachment to be realistic.
4. The effect of the Reynolds stresses in the outer part of the re-attaching shear layer can be assumed to remain constant at the free shear-layer value.
5. The effect of the wall shear stress during the process of readjustment is negligible.

The work reported in this note was performed in part fulfilment of Ministry of Aviation Contract No. KU/4/025/CB 53 (*a*) and the author is indebted to the Ministry for permission to publish.

REFERENCES

BEASTALL, E. & EGGINK, H. 1951 *R.A.E. Tech. Note Aero.* no. 2061.

CHAPMAN, D. R., WIMBROW, W. R. & KESLER, R. H. 1952 *NACA T.N.* no. 2611.

CHAPMAN, D. R., KUEHN, D. M. & LARSON, H. K. 1959 *NACA Rep.* no. 1356.

COOKE, J. C. 1963 *R.A.E. Note Aero.* no. 2879.

GADD, G. E., HOLDER, D. W. & REGAN, J. D. 1955 *Aero. Res. Counc.* **17**, 490.

GOIN, K. L. 1952 *NACA R.M.* L52D21.

HASTINGS, R. C. 1963 *R.A.E. Tech. Note Aero.* no. 2931.

HONDA, M. 1958 *J. Aero. Sci.* **25**, 667.

KIRK, F. N. 1959 *R.A.E. Tech. Note Aero.* no. 2377.

KORST, H. H., PAGE, R. H. & CHILDS, M. E. 1955 University of Illinois ME-TN-392-3.

KORST, H. H., CHOW, W. L. & ZUMWALT, G. W. 1959 University of Illinois ME-TN-392-5.

LIEPMANN, H. W. & LAUFER, J. 1947 *NACA T.N.* no. 1259.

LOVE, E. S., 1957 *NACA T.N.* no. 3819.

LUDWIEG, H. & TILLMAN, W. 1950 *NACA T.M.* no. 1285.

MAGER, A. 1956 *J. Aero. Sci.* **23**, 181.

MAGER, A. 1959 *J. Aero. Sci.* **25**, 305.

MASKELL, E. C. 1951 *R.A.E. Rep. Aero.* no. 2443.

MCCULLOUGH, G. & GAULT, D. 1949 *NACA T.N.* no. 1923.

MCDONALD, H. 1964 *Aero. Quart.* **15**, 247.

MORROW, J. D. & KATZ, E. 1955 *NACA T.N.* no. 3548.

MUELLER, T. J. & ROBERTSON, J. M. 1963 *Modern Developments in Theoretical and Applied Mechanics*, vol. I, p. 326.

NASH, J. F. 1962*a* *N.P.L. Aero Rep.* no. 1019.

NASH, J. F. 1962*b* *N.P.L. Aero. Rep.* 1036 (*R. & M.* no. 3344).

NASH, J. F. 1964 *N.P.L. Aero. Rep.* no. 1112.

NASH, J. F., QUINCEY V. G. & CALLINAN, J. 1963 *N.P.L. Aero. Rep.* no. 1070.

RAY, A. K. 1962 *Z. Flugwiss.* **10**, Heft 6.

RESHOTKO, E. & TUCKER, M. 1955 *NACA T.N.* no. 3454.

RESHOTKO, E. & TUCKER, M. 1957 *NACA T.N.* no. 4154.

SALTZMAN, E. J. 1961 *NASA T.N.* D-1056.

SANDERS, F. & CRABTREE, L. F. 1963 *R.A.E. Tech. Note Aero.* no. 2751.

SIRIEUX, M. 1960 *La Recherche Aeronautique*, Sept./Oct.

SQUIRE, H. B. & YOUNG, A. D. 1937 *Aero. Res. Counc. R. & M.* 1838.

STRATFORD, B. S. 1959 *J. Fluid Mech.* **5**, 1.

TETERVIN, N. & LIN, C. C. 1951 *NACA Rep.* no. 1046.

TOWNSEND, A. A. 1960 *J. Fluid Mech.* **8**, 143.

TOWNSEND, A. A. 1962 *J. Fluid Mech.* **12**, 536.

WHITE, R. A. 1963 University of Illinois Ph.D. Thesis.

WIMBROW, W. R. 1954 *NACA* A54A07.

Appendix 1. Some relationships under the Mager transformation

It can fairly readily be shown that using the transformation of Mager (1959) the following relationships hold

$$\delta = \{1+\tfrac{1}{2}(\gamma-1)M_e^2\}^3\bar{\delta}^* + \tfrac{1}{2}(\gamma-1)M_e^2\{1+\tfrac{1}{2}(\gamma-1)M_e^2\}^3(\bar{\theta}^*+\bar{\Delta}^*), \quad (A\,1.1)$$

$$\theta = \{1+\tfrac{1}{2}(\gamma-1)M_e^2\}^3\bar{\theta}^*, \quad (A\,1.2)$$

$$H = \{1+\tfrac{1}{2}(\gamma-1)M_e^2\}\bar{H}^* + \tfrac{1}{2}(\gamma-1)M_e^2, \quad (A\,1.3)$$

$$\Delta = \{1+\tfrac{1}{2}(\gamma-1)M_e^2\}^4\bar{\Delta}^* + \tfrac{1}{2}(\gamma-1)M_e^2\{1+\tfrac{1}{2}(\gamma-1)M_e^2\}^3\bar{\theta}^*. \quad (A\,1.4)$$

Hence, after some manipulation,

$$\frac{\theta}{\delta} = \frac{\bar{\theta}^*/\bar{\delta}^*}{1+\tfrac{1}{2}(\gamma-1)M_e^2(\bar{\theta}^*/\bar{\delta}^*+\bar{\Delta}^*/\bar{\delta}^*)}, \quad (A\,1.5)$$

$$\frac{\Delta}{\delta} = \frac{(1+\tfrac{1}{2}(\gamma-1)M_e^2)\bar{\Delta}^*/\bar{\delta}^* + \tfrac{1}{2}(\gamma-1)M_e^2\bar{\theta}^*/\bar{\delta}^*}{1+\tfrac{1}{2}(\gamma-1)M_e^2(\bar{\theta}^*/\bar{\delta}^*+\bar{\Delta}^*/\bar{\delta}^*)}. \quad (A\,1.6)$$

Appendix 2. The wall shear stress contribution to the change in boundary-layer thickness parameters downstream of the re-attachment point

Tetervin & Lin (1951) give the momentum integral equation and the moment-of-momentum equation of an incompressible boundary layer as

$$\frac{d\theta}{dx}+\frac{\theta}{u_e}(H+2)\frac{du_e}{dx} = \frac{\tau_w}{\rho u_e^2}, \quad (A\,2.1)$$

$$\theta\frac{dH}{dx} = -\frac{H(H+1)(H^2-1)}{2}\frac{\theta}{u_e}\frac{du_e}{dx} + H(H^2-1)\frac{\tau_w}{\rho u_e^2} - (H+1)(H^2-1)\int_0^1 \frac{\tau}{\rho u_e^2}\,d\left(\frac{y}{\delta}\right), \quad (A\,2.2)$$

neglecting the normal stress and pressure variation terms.

Equations (A 2.1) and (A 2.2) provide two relationships between five unknowns, the momentum thickness θ, the shape parameter H, the free-stream velocity distribution u_e, the wall shear stress τ_w and the shear distribution across the layer τ. Following standard boundary-layer practice some relationship between θ, H and τ_w could be adopted such as the Ludwieg–Tillmann (1950) relationship. Another relationship is readily supplied by linear supersonic-flow theory, which relates the growth of the displacement thickness to the change in pressure (this statement implies that equations (A 2.1) and (A 2.2) are the transformed equations of some supersonic interaction). Finally to completely determine the solution it only remains to relate the local shear-stress distribution to θ, H and τ_w. Leaving aside that problem for the moment, Reshotko & Tucker (1957) have integrated (A 2.2) to give

$$f(H)/f(H_4) = (u_e/u_{e4})\,e^{-\xi(x)}, \quad (A\,2.3)$$

where

$$\xi(x) = \int_{x_4}^{x}\left[\frac{C_f}{(H+1)\theta} - \frac{1}{H\theta}\int_0^1 \frac{\tau}{\tfrac{1}{2}\rho u_e^2}\,d\left(\frac{y}{\delta}\right)\right]dx, \quad (A\,2.4)$$

and $f(H)$ is defined by (4). It is worth noting that the result used earlier from Reshotko & Tucker (1955) to determine the condition of the boundary layer at

separation; that is equations (3) to (6) are obtained from (A 2.3) and (A 2.1) on assumption that $\xi(x)$ and τ_w are negligible. In the present case of flow re-attachment, however, $\xi(x)$ cannot be negligible, for it is this term which opposes the pressure-gradient effect on the shape parameter and permits the flow to re-attach. (In McDonald 1964) an estimate of $\xi(x)$ was obtained using the semi-empirical wake recompression of law of Squire & Young.) It remains to show that the effect of the wall shear stress on the thickness calculation is negligible even when the re-attachment length is not small, thus enabling the method of McDonald (1964) to be used in this case.

This is done by returning to the concept of an inner and outer layer and noting that in the outer layer the boundary layer will not be greatly affected by the wall. Thus the change in the integral of local shear accross the boundary layer will be restricted mainly to the region close to the wall. Supposing this inner layer to extend out to half the boundary-layer thickness allows a rough estimate of about $\frac{1}{3} C_f$ to be made for the maximum value of the difference in shear integral between wall and wake re-attachment. In this fashion the difference in $\xi(x)$ can be expressed in the form

$$\xi(x)_{\text{wall}} - \xi(x)_{\text{wake}} = \int \left[\frac{1}{H+1} - \frac{1}{3H}\right] \frac{C_f}{\theta} dx \qquad \text{(A 2.5)}$$

and it is a straightforward matter to demonstrate that this integral is of order 10^{-3} for the very long re-attachment lengths of Mueller & Robertson (1963) and McCullough & Gault (1949). Since $\xi(x)$ must be of order unity (McDonald 1964) the difference between wall and wake recompression is therefore shown to be very small in so far as the shape parameter H is concerned.

In a similar fashion it is not difficult to show that integrating the momentum equation with and without the wall shear stress yields very similar results for the experiments of Mueller & Robertson (1963) and from this it would seem that in the present circumstances it is permissible to neglect the wall shear stress contribution to the change in boundary-layer thickness parameters, and so use the method of McDonald (1964).